NUMERICAL SIMULATION OF ICE ACCRETION ON AIRFOIL

Dr. math. Maria ALEXANDRESCU, Phys. Nicusor ALEXANDRESCU, malex@incas.ro

DOI: 10.13111/2066-8201.2009.1.1.4

Abstract

This work consists in the simulation of the ice accretion in the leading edge of aerodynamic profiles and our proposed model encompasses: geometry generation, calculation of the potential flow around the body, boundary layer thickness computation, water droplet trajectory computation, heat and mass balances and the consequent modification of the geometry by the ice growth. The flow calculation is realized with panel methods, using only segments defined over the body contour. The viscous effects are considered using the Karman-Pohlhausen method for the laminar boundary layer. The local heat transfer coefficient is obtained by applying the Smith-Spalding method for the thermal boundary layer. The ice accretion limits and the collection efficiency are determined by computing water droplet trajectories impinging the surface. The heat transfer process is analyzed with an energy and a mass balance in each segment defining the body. Finally, the geometry is modified by the addition of the computed ice thickness to the respective panel. The process by repeating all the steps. The model validation is done using a selection of problems with experimental solution, CIRA (the CESAR project). Hereinafter, results are obtained for different aerodynamic profiles, angles of attack and meteorological parameters.

Introduction

Problem description and assumptions

The first stage in any icing analysis is to determine where and at what rate the cloud water droplets are deposited on the surface of the body (e.g. wing or fuselage) under investigation. This characteristic is frequently referred to as the water-collection or catch-efficiency distribution. The local value of catch efficiency represents the fraction of the freestream water concentration which impacts at a given surface location of the body. The distribution normally has a peak close to the aerodynamic stagnation point and reduces in value to zero at some aft location usually on each of the upper and lower surfaces of the body (aerofoil). Typical peak values range from *ca*. 90% for a rotor with small chord (less than or equal to 0.75 m) and high speed (200 m s¡1) to 50% peak or less for large chord wings (greater than or equal to 2 m) at typical speeds of commercial transport aircraft during hold (e.g. 75-140 m s^{-1}).

There are two main types of trajectory calculation in use today. The first and most frequently adopted method is a traditional Lagrangian formulation in which the trajectory of an individual water droplet is tracked from a specified starting point upstream of the body (usually five to seven chord lengths ahead of the body). The second and more recently adopted approach is Eulerian, in which the volume fraction is computed at the same node positions at which the aerodynamic parameters are known. No individual particles are therefore tracked in this approach and the answer leads directly to a measure of the catch efficiency. For both methods, either a flow solution or a means of calculating the aerodynamic flow is necessary. Methods adopted depend on the application and range from simple panel methods through to full Navier-Stokes solvers.

Water droplet trajectory calculations

The derivation of the equation for the droplet acceleration in the x-direction is shown below. The derivation for the acceleration in the y- and z-directions for three dimensional calculations is very similar and therefore not shown. The primary assumptions on which the equations are based are as follows.

(1) The droplets are spherical and do not deform.
(2) There is no collision or coalescence of droplets.
(3) Turbulence effects may be neglected.
(4) The only forces acting on the droplet are due to aerodynamic drag, gravity and buoyancy.
(5) The water droplet concentration is sufficiently small for the droplets to have a negligible effect on the aerodynamic flow and therefore the air flow and water droplets may be treated as independent systems.

An illustration of the coordinate system and terminology employed in this note for the aerofoil and droplet is provided in figures 1 and 2.In case of a single particle, where V_a is the local air velocity, u_a is the local air velocity component in the x-direction, v_a is the local air velocity component in the y-direction, V_d is the droplet velocity, u_d is the droplet velocity component in the x-direction, v_d is the droplet velocity component in the y-direction, u_{rel} is the relative air/droplet velocity in the x-direction, v_{rel} is the relative air/droplet velocity, V_{res} is the resultant of the relative velocities u_{rel} and v_{rel}, the aerodynamic force on the droplet, F_a, is

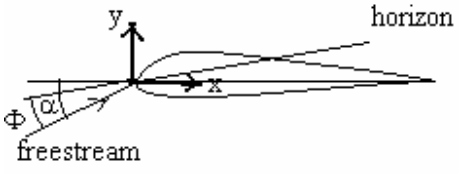

Fig.1 Velocity ccomponent definition

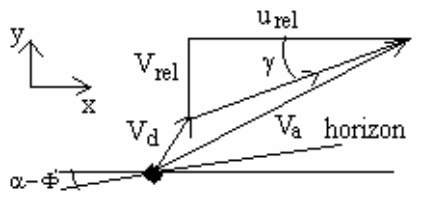

Fig.2 Trajectory coordonate system definition in the y-direction,

$$F_a = \frac{1}{2} C_D \rho_a A_d V_{res}^2 \tag{1}$$

The component of this force acting in the x-direction is

$$\begin{aligned} F_{ax} &= \frac{1}{2} C_D \rho_a A_d V_{res}^2 \cos\gamma \\ &= \frac{1}{2} C_D \rho_a A_d V_{res} u_{rel} \end{aligned} \tag{2}$$

Taking u_d as the component of the droplet velocity in the x-direction, F_{ax} as the component of the aerodynamic force in the x-direction, F_{gx} as the component of the gravitational force in the x-direction, A_d as the frontal area of the droplet,Das the droplet diameter,g as the acceleration due to gravity, ρ_d as the droplet density (1000 kg m^{-3} for water), ρ_a as the air density, m_d as the droplet mass, c as the aerofoil chord, C_D as the drag coefficient for the droplet, the following expression for the acceleration in the x-direction (in m s^{-1}) may be derived:

$$\frac{du_d}{dt} = \frac{F_{ax} + F_{gx}}{m_d} \tag{3}$$

Using the following expressions,

$$m_d = \rho_d \times \frac{4}{3}\pi\frac{1}{8}D^3$$

$$A_d = \frac{1}{4}\pi D^2,$$

$$F_{gx} = m_d g\left(1 - \frac{\rho_a}{\rho_d}\right)\sin(\alpha - \phi), \tag{4}$$

$$\frac{du_d}{dt} = \frac{\frac{1}{2} C_D \rho_a \pi \frac{1}{4} D^2 V_{res} u_{rel}}{\frac{4}{24}\rho_d \pi D^3} +$$

$$\frac{m_d g}{m_d}\left(1 - \frac{\rho_a}{\rho_d}\right)\sin(\alpha - \phi)$$

This can be further simplified by making a substitution using the droplet Reynolds number

$$R = \frac{\rho_a V_{res} D}{\mu} \tag{5}$$

$$\frac{du_d}{dt} = \frac{18 C_d R \mu u_{rel}}{24\rho_d D^2} + \left(1 - \frac{\rho_a}{\rho_d}\right) g \sin(\alpha - \phi) \tag{6}$$

which are written in a non-dimensional form using

$$\bar{u}_d = \frac{u_d}{V_\infty}, \quad \bar{t} = \frac{tV_\infty}{c}, \quad \bar{u}_{rel} = \frac{u_{rel}}{V_\infty}$$

$$\frac{d\bar{u}_d}{dt} \times \frac{V_\infty^2}{c} = \frac{18 C_d R \mu \bar{u}_{rel} V_\infty}{24\rho_d D^2}$$

$$+\left(1 - \frac{\rho_a}{\rho_d}\right) g \sin(\alpha - \phi) \quad \textit{astfel ca}$$

$$\frac{d\bar{u}_d}{dt} = \frac{18 C_d R \mu \bar{u}_{rel}}{24\rho_d D^2 V_\infty}$$

$$+\left(1 - \frac{\rho_a}{\rho_d}\right)\frac{c}{V_\infty^2} g \sin(\alpha - \phi). \tag{7}$$

Similarly,

$$\frac{d\bar{v}_d}{dt} = \frac{18 C_d R \mu \bar{v}_{rel}}{24\rho_d D^2 V_\infty}$$

$$-\left(1 - \frac{\rho_a}{\rho_d}\right)\frac{c}{V_\infty^2} g \cos(\alpha - \phi).$$

Furthermore, introducing the inertia parameter

$$K = \frac{\rho_d D^2 V_\infty}{18\mu c}$$

result

$$\frac{d\bar{u}_d}{d\bar{t}} = \frac{C_d R \bar{u}_{rel}}{24K}$$

$$+\left(1 - \frac{\rho_a}{\rho_d}\right)\frac{c}{V_\infty^2} g \sin(\alpha - \phi) \tag{8}$$

$$\frac{d\bar{v}_d}{d\bar{t}} = \frac{C_d R \bar{v}_{rel}}{24K}$$

$$-\left(1 - \frac{\rho_a}{\rho_d}\right)\frac{c}{V_\infty^2} g \cos(\alpha - \phi)$$

The equations of motion are readily solved using Runge-Kutta or similar numerical methods, with the initial droplet velocity at the trajectory starting point several chord lengths ahead of the body usually assumed to be the same as that of the aerodynamic flow.

Flow solution

With panel methods, the flow solution is evaluated at each position of the droplet trajectory by

summing the contribution to the flow from the calculated circulation from a series of panels that describe the aerofoil or body profile. The flow solution at the surface of the profile is also required in the accretion analysis.

The alternative is a grid-based solution in which the velocity is known at discrete node points of a grid around the body. The velocity at a given point in space is then estimated by interpolation using the surrounding grid nodes.

We consider a control volume located on the surface of the body and which extends from outside the boundary-layer to the surface.

The lower boundary of the control volume is initially on the surface of the clean geometry and moves outward with the surface as the ice accretes. Computationally a control volume is placed over each panel defining the body geometry as shown in fig 3.

The conservation of mass requires that the mass flow rate entering the control volume is equal to the mass flow rate leaving the control volume, that is:

$$\dot{m}_C + \dot{m}_{r_{in}} = \dot{m}_i + \dot{m}_e + \dot{m}_{r_{outt}} \qquad (9)$$

Here $\dot{m}_C$ is the mass flow rate of the impinging water entering the control volume and $\dot{m}_{r_{in}}$ is the mass flow rate of the water along the surface exiting from the adjacent upstream control volume. The leaving mass flow rates consist of the "accumulated ice", $\dot{m}_i$, loss through evaporation, $\dot{m}_e$, and water flowing out of the control volume, $\dot{m}_{r_{out}}$ .The three mass flow rates $\dot{m}_i$, $\dot{m}_C$, and $\dot{m}_{in}$ are related to each other by the concept of freezing factor f, defined as the fraction of the total mass flow rate of water entering the control volume that freezes,

$$f = \frac{\dot{m}_i}{\dot{m}_{Ci} + \dot{m}_{r_{in}}} \qquad (10)$$

Solving for $\dot{m}_i$ and substituting the resulting expression into the value of $\dot{m}_{r_{out}}$ can be obtained from:

$$\dot{m}_{out} = \left(\dot{m}_C + \dot{m}_{r_{in}}\right)(1 - f) - \dot{m}_e \qquad (11)$$

once f, $\dot{m}_C$, $m_{r_{in}}$ *and* $\dot{m}_e$ are known.

The equation (11) is applied to each surface element on the airfoil where ice accumulates. Calculations start from the stagnation point where $\dot{m}_{in} = 0$, because of symetry and proceed in the downstream direction on both upper and lower surfaces.

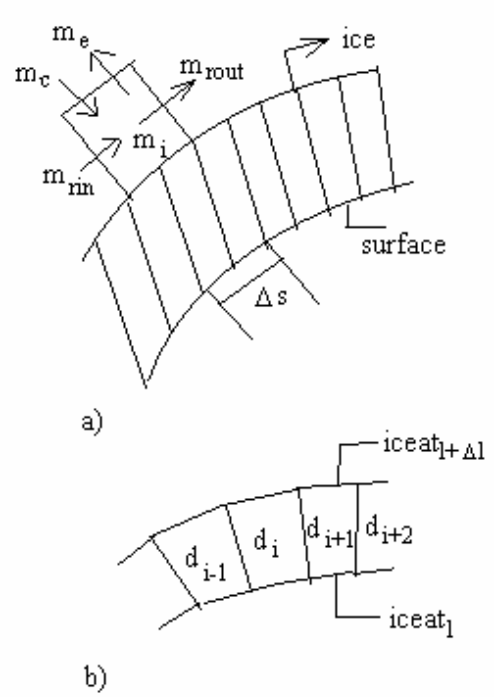

Fig.3.Control volume for the energy balance (a) single control volume on the icing surface, (b) control volumes over each panel which defines the airfoil geometry

At the first surface element, for an assumed f, equation (11)contains only one unknown quantity, which is $\dot{m}_{r_{out}}$ since $\dot{m}_C$ is computed from coresponding equations [1]. At the next surface element $\dot{m}_{r_{out}}$ of the first segment becomes $\dot{m}_{in}$ for the second segment and with $\dot{m}_C$ and $\dot{m}_e$ computed [1] as before, $\dot{m}_{r_{out}}$ is computed from eq. 11 and this process is repeated for each surface segment.

The energy balance is applied to the control volume by using the first law of thermodynamics which requires that the energy inflow rate is equal to the energy outflow rate.

Application of the energy balance to the control volume of Fig.3 gives:

$$\dot{m}_C H_{t,T_\infty} + \dot{m}_{r_{in}} H_{w,s_{i-1}} + \dot{q}_k \Delta s = \dot{m}_e H_{v,s} + \dot{m}_e H_{i,s} + \dot{m}_{ext} H_{w,s_i} + \dot{q}_C \Delta s \qquad (12)$$

The equations (11) and (12) are solved iteratively.

The thickness of boundary ice is:

$$\Delta y = \frac{\dot{m}_i}{\rho_i} \qquad (13)$$

These Δy increments are then added to the original surface segments as to create a new airfoil on which the ice accumulation calculations are repeated for the Δt next time interval.

Thus, calculations for each step involves recomputing the inviscid flow, determining impingement pattern for the new configuration, and reevaluating the heat balance equation. Numerical calculation includes the phases:

1) read the intial coordinates, x,z, of the considered airfoil profile and the speed distribution U_e is computed for the airfoil with the panels method;
2) the dynamical and thermal boundary layer equations are solved, resuting:

$$\overline{U} \text{ and } \overline{\Delta T};$$

3) with (5.16) the ice thickness for the first time step is calculated;
4) the new coordinates of airfoil profile are calculated;

The (1) step is repeated.

Conclusions

The phenomenon of ice accretion over the airfoil profile is the effect of a triplet : the mass of water droplets (from cloud),the air fluid motion over the airfoil profile and the solid surface. These interactions are controled by many factors, who are defined as parameter:

- the pression, the temperature and humidity of the environment.
- the speed and direction of air stream ;
-the physical and chemical of cloud mass (the density and chemical composition of cloud)
-the interaction between water droplet and airstream (the buoyancy force, the friction force) that are determined by V_∞, ρ_d, K.
-the interaction between the water droplets and the phenomenon from dynamic and thermal boundary layer ($U_e, \overline{U}, \overline{\Delta T}$), the mass and energy transfer, free and forced convection;
-the interaction between the droplets and the solid surface of the airfoil profile semi-elastic interaction (the efficiency of droplets adhesion at the airfoil surface.

With the considered mathematical model, a numerical code simulating the process of ice accretion over the airfoil is elaborated. The form and mass of ice deposition over the aerodynamic airfoil are functions of R_d/ R_∞, τe = b/a, α=0. The calculation is done for laminar and incompressible flow around the aerodymamic profiles described in Anexe 1 and the results are represented in the following figures in Anexe 2:

Fig.1 R_d/R_∞ : (0.45, 0.55, 0.65, 0.75, 0.85, 0.95); τ = 0.25; e = b/a : (1, 0.5, 0.25, 0.125)

Fig. 2 τ : (0.01, 0.05, 0.1, 0.15, 0.2, 0.25), R_d/R_∞ = 0.85, e = b/a : (1, 0.5, 0.25, 0.125)

Fig.3 ΔT: (0.005, 0.1, 0.3, 0.5, 0.7) ; Rd/R_∞ = 0.85; e = b/a : (1, 0.5, 0.25, 0.125)

Fig.4 $\overline{U}$ the influence of dynamic and thermal boundary layer $\overline{\Delta T}$, about ice acretion simulation τ : (0.01, 0.05, 0.1, 0.15, 0.2, 0.25) R_d/R_∞ = 0. 85.

Fig.5 The simultaneous influence of Kr (roughness), $\overline{U}$, of dynamic and thermal boundary layer $\overline{\Delta T}$; τ : (0.01, 0.05, 0.1, 0.15, 0.2, 0.25), R_d/R_∞ = 0.85.

Fig.6 The simultaneous influence of Kr (roughness), $\overline{U}$, of dynamic and thermal boundary layer $\overline{\Delta T}$ for aerodynamic profiles; τ : (0.01, 0.05, 0.1, 0.15, 0.2, 0.25) , R_d/R_∞ = 0.85.

REFERENCES

[1] *CEBECI, T.,* ***"An Engineering Approach to the calculation of Aerodynamic Flows";*** Springer, 1999.

[2] *R.W. GENT, N.P. DART and J.T. CANSDALE,* ***"Aircraft Icing",*** Phil. Trans. R. Soc. London A (2000) 358, 2873-2911.

[3] *SANDER J. JACOBS, JACCO M. HOSPERS, HARRY W.M. HOEIJMAKERS*, University ofTwente Enschede, the Netherlands, 26TH International Congress of the Aeronautical Sciences, 2008.

Anexa I

Thin profile

$$z(x) = h\begin{pmatrix} 0.1969\sqrt{x} - 0.126x - \\ 0.2537x^2 + 0.2843x^3 \\ -0.1015x^4 \end{pmatrix}$$

for h=1.

$$z(x) = -h\begin{pmatrix} 0.2969\sqrt{x} - \\ 0.226x - 0.4537x^2 + \\ 0.4843x^3 - 0.1015x^4 \end{pmatrix}$$

for h=1.

Thick profile

$$z(x) = h\begin{pmatrix} 0.2969\sqrt{x} - 0.126x \\ -0.3537x^2 + 0.2843x^3 \\ -0.1015x^4 \end{pmatrix}$$

$$z(x) = h\begin{pmatrix} 0.4969\sqrt{x} - 0.426x \\ -0.4537x^2 + 0.4843x^3 \\ -0.1015x^4 \end{pmatrix}$$

Anexa II

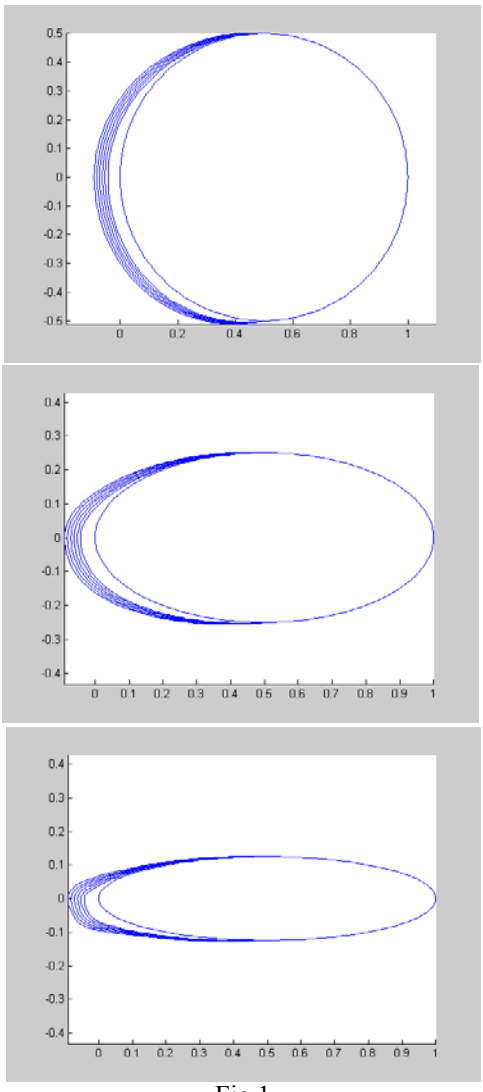

Fig.1

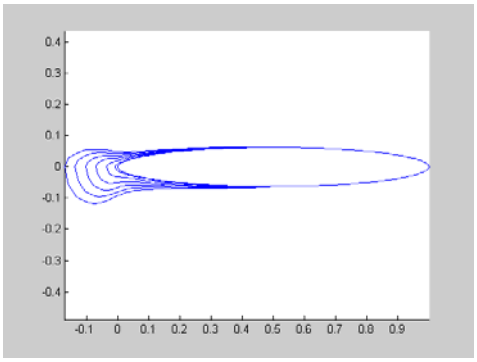

Fig.2

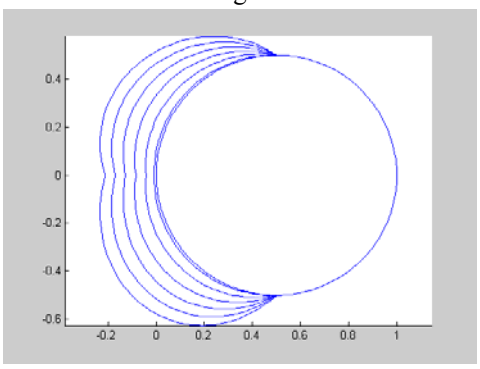

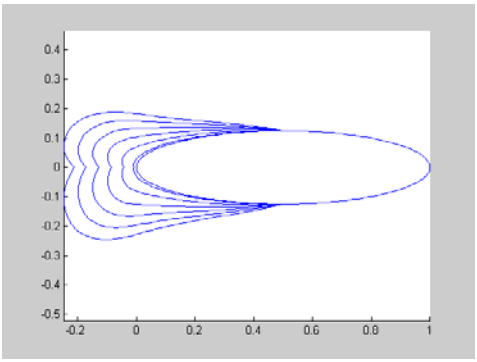

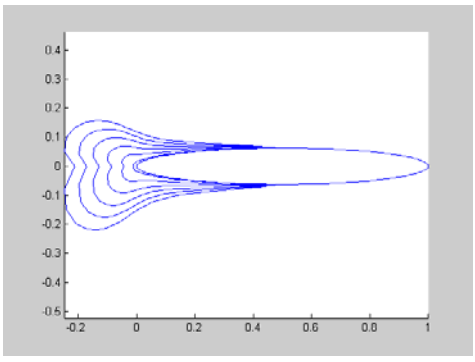

Fig.3

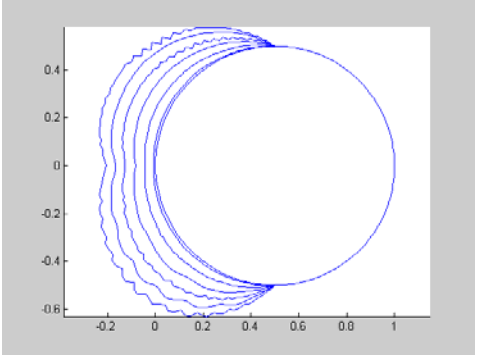

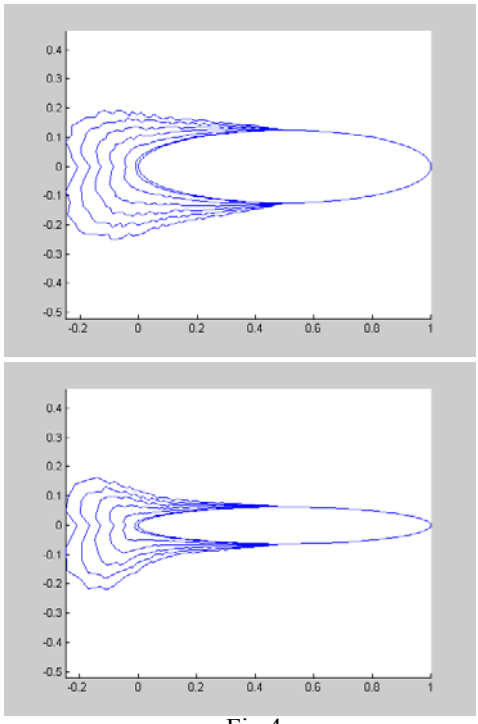

Fig.4

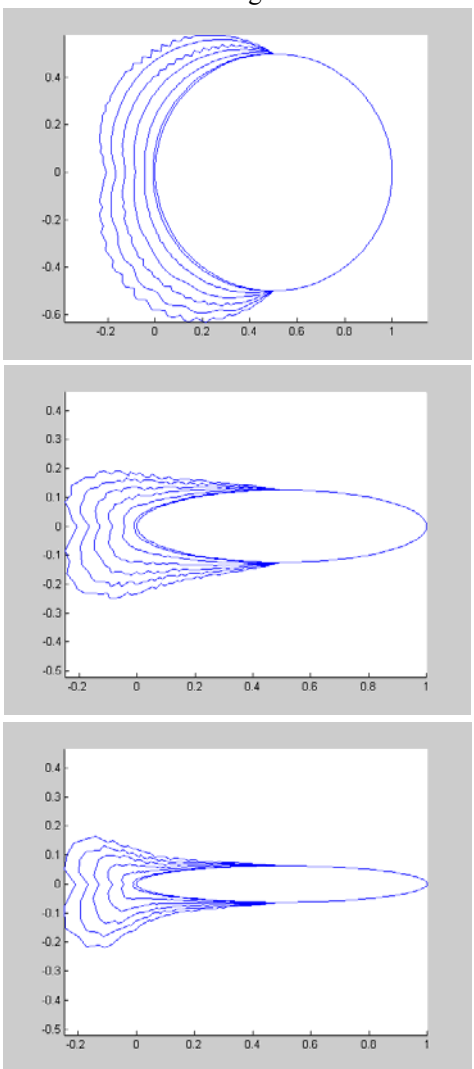

Fig.5

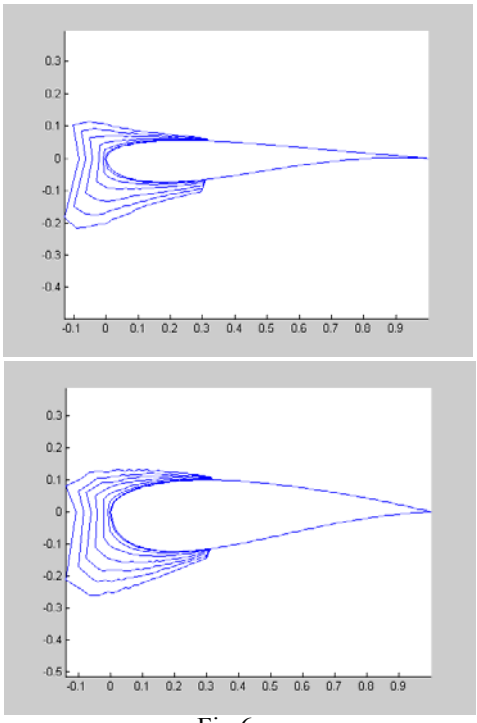

Fig.6